JOURNAL OF CATALYSIS 139, 444–454 (1993)

CO Hydrogenation on PdCo/NaY Catalysts: Effect of Ion Hydration on Metal Phases and Selectivity

YUAN-GEN YIN ZONGCHAO ZHANG, AND WOLFGANG M. H. SACHTLER[1]

V. N. Ipatieff Laboratory, Center for Catalysis and Surface Science, Northwestern University, Evanston, Illinois 60208

Received July 13, 1992; revised September 8, 1992

Exposure of calcined PdCo/NaY catalyst precursors to water vapor, prior to reduction, strongly affects the CO hydrogenation activity and selectivity of the reduced bimetal catalysts. With samples that had been exposed to H_2O before reduction, the formation of hydrocarbons prevails; nonhydrated reference samples of the same overall composition are mainly selective for oxygenates. After 6 h of reaction time PdCo alloy particles of 5.8 nm are detected by XRD in H_2O-exposed catalysts, but in the reference samples the metal particles are below the limit of detection by XRD. The observed effects are attributed to the formation of mobile aequo-complexes of metal ions; after reduction they are converted to larger alloy particles, richer on Co, than in the reference samples. Results obtained with NaOH-neutralized and Co-free Pd/NaY catalysts are also discussed.

I. INTRODUCTION

Combinations of Group VIII metals, either as alloys or as metal-ion adducts, have often been found to display catalytic performances which strongly differ from those of the individual metal components or their physical mixtures. Examples reported in the literature include combinations of Mn with Rh (*1*, *2*) and Fe with noble metals, e.g., IrFe (*3*) and PdFe (*4*, *5*). Zeolite supports have the advantage of entrapping very small metal clusters, but often the reduction of ions such as Fe^{2+}, Co^{2+}, or Ni^{2+} is more difficult in zeolites than on amorphous supports (*6*, *7*). Recently we reported that the presence of a noble metal in the same zeolite can enhance the reduction of ions of a less reducible element (*8–10*). A condition is that those ions are in close proximity to either the ions or the reduced nuclei of the more noble element.

In a recent paper on CO hydrogenation with PdCo/NaY catalysts (*11*), we reported on the effect of relative metal loadings on the catalytic performance. The activities and selectivities of those catalysts were correlated with the metal and carbide phases identified by X-ray diffraction. In the present research we varied another experimental parameter which was found to have a rather dramatic effect on the catalyst performance: exposure to water vapor of the calcined catalyst precursors prior to reduction.

II. EXPERIMENTAL

All Pd_9Co_9/NaY catalysts (subscripts indicating atoms per unit cell) were prepared by successive ion-exchange of NaY (LZ Y-52) as described elsewhere (*9*). Two calcination/reduction programs were used: T_C = 500°C, T_R = 250°C; and T_C = 500°C, T_R = 500°C, where T_C and T_R stand for the ultimate temperatures of the calcination and reduction programs. Calcination was conducted in an O_2 stream (>1000 $cm^3\ s^{-1}$ (g catalyst)$^{-1}$) with a heating rate of 0.5 K min; at 500°C the sample was held for 2 h. Reduction was carried out in a flow (>20 $cm^3 s^{-1}$) of ultra-high purity H_2. Two series of catalysts were tested for CO hydrogena-

[1] To whom correspondence should be addressed.

0021-9517/93 $5.00

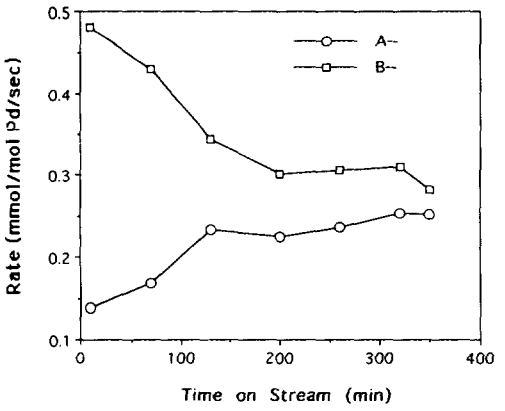

FIG. 1. Change in conversion rate of CO hydrogenation over Pd_9Co_9 500/H_2O/250 and 500/250 catalysts versus time on stream: (A) 500/H_2O/250 and (B) 500/250.

tion: (I) $T_C/H_2O/T_R$ samples that were exposed, between calcination but before reduction, to air saturated with H_2O above a saturated aqueous solution of NH_4Cl for more than 1 day; (II) T_C/T_R samples that were calcined and reduced without intermediate rehydration. The T_C/T_R catalysts were sealed in a glass reactor with teflon stopcocks after reduction and discharged under dry He atmosphere into a small tared vial flushed with dry He in a glove bag. In a third group of samples a Pd_9Co_9/NaY catalyst, after calcination and reduction at 500°C, was transferred to a glove bag and neutralized with an ample volume of aqueous NaOH (pH = 10.5) under a He atmosphere. These catalysts are termed 500/500/NaOH. Weighed samples of (II) were transferred into a microreactor inside the glove bag. In an effort to minimize air exposure the loaded microreactor was subsequently mounted within 5 min into the Xytel system (*12*). After flushing with He for 5 min, the catalyst was heated up in hydrogen stream to the reaction temperature.

The effect of alloying Co with Pd was studied by comparing the Pd_9Co_9 catalyst with a Pd_9 catalysts calcined and reduced at 500°C, with or without intermediate rehydration. CO hydrogenation was conducted with 0.3–0.8 g. of catalyst in the Xytel system (Max II) at 250°C and 10 bar, with total syngas (H_2/CO = 1) space velocity of about 3600–4000 h^{-1}; conversion was kept below 1%. The product effluent was analyzed with an on-line HP-5890A gas chromatograph, equipped with a cross-linked methyl silicone capillary column (0.2 mm diameter, 50 m length) and FID. Helium was used as carrier gas. Catalyst activity is expressed as conversion rate of CO in mmol/mol Pd/sec, selectivity in % mol C (denotes formation of CH_4, oxygenates, and heavier hydrocarbons), and hydrocarbon distribution in % mol C.

X-ray diffraction of catalysts at various stages of reaction was conducted and analyzed as described in (*11*), where also the assignment of peaks was described.

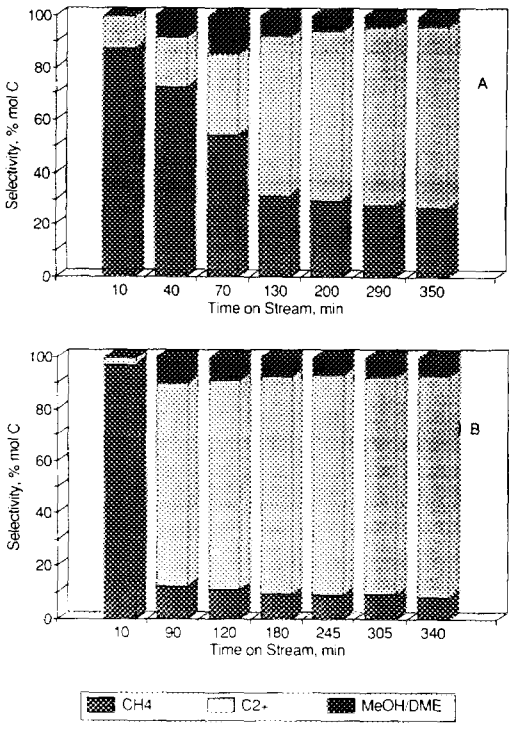

FIG. 2. Change in selectivity of CO hydrogenation over Pd_9Co_9 500/H_2O/250 and 500/250 catalysts versus time on stream: (A) 500/H_2O/250 and (B) 500/250.

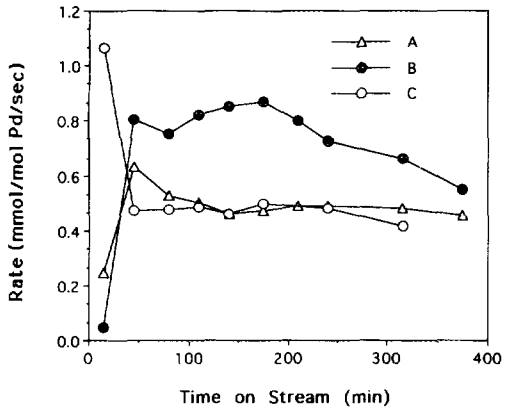

FIG. 3. Change in conversion rate of CO hydrogenation over Pd_9Co_9 500/H_2O/500, 500/500, and 500/500/NaOH catalysts versus time on stream: (A) 500/H_2O/500, (B) 500/500, and (C) 500/500/NaOH.

III. RESULTS

a. 500/H_2O/250 and 500/250 Catalysts

As shown in Fig. 1, the activity of catalyst 500/H_2O/250 is initially lower than that of 500/250, but in the steady state the difference is much smaller. Both catalysts show a high initial selectivity for methane (Fig. 2), but in the steady state heavier hydrocarbons (C_2- hereafter) prevail, in particular the 500/250 catalysts produces significant amounts of C_{4+} hydrocarbons. During longer reaction times, up to 25 h, activity and selectivity of these catalysts remain almost constant.

b. 500/H_2O/500 and 500/500 Catalysts

The change of activity with reaction time follows a similar pattern for the 500/H_2O/500 and 500/500 catalysts as shown in Fig. 3. However, in the steady state 500/500 is remarkably more active than 500/H_2O/500. The most intriguing result is the dramatic difference in selectivity. While the 500/H_2O/500 catalyst produces methane and other hydrocarbons, the 500/500 catalyst shows, after a short induction period, a high selectivity to the oxygenates methanol and dimethylether (MeOH + DME hereafter), as shown in Fig. 4. After 22 h on stream, the activity of this catalyst has dropped to about 1/30 of its maximum activity; concomitantly its selectivity for oxygenates diminishes. Figure 5 shows a change in hydrocarbon distribution for these catalysts. Changes in the methanol/dimethyl ether ratio are shown in Fig. 6.

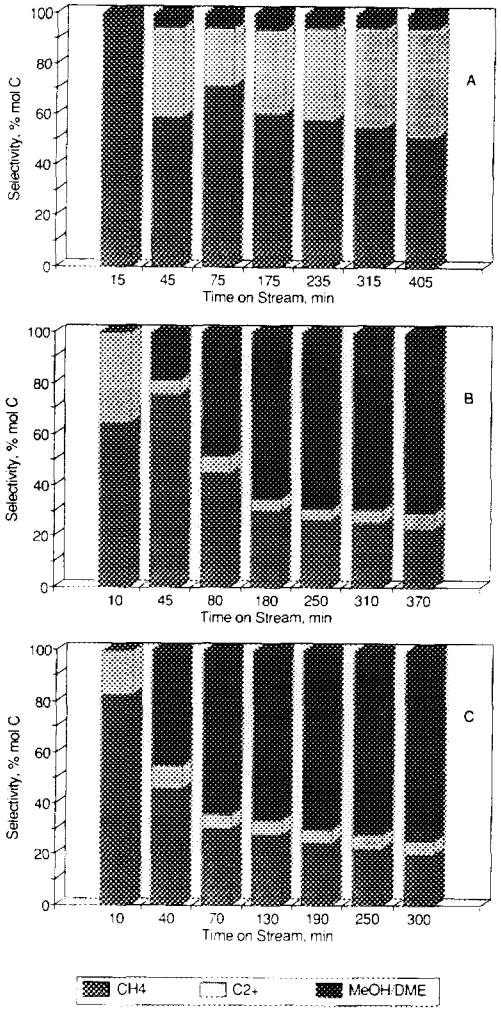

FIG. 4. Change in selectivity of CO hydrogenation over Pd_9Co_9 500/H_2O/500, 500/500, and 500/500/NaOH catalysts versus time on stream: (A) 500/H_2O/500, (B) 500/500, and (C) 500/500/NaOH.

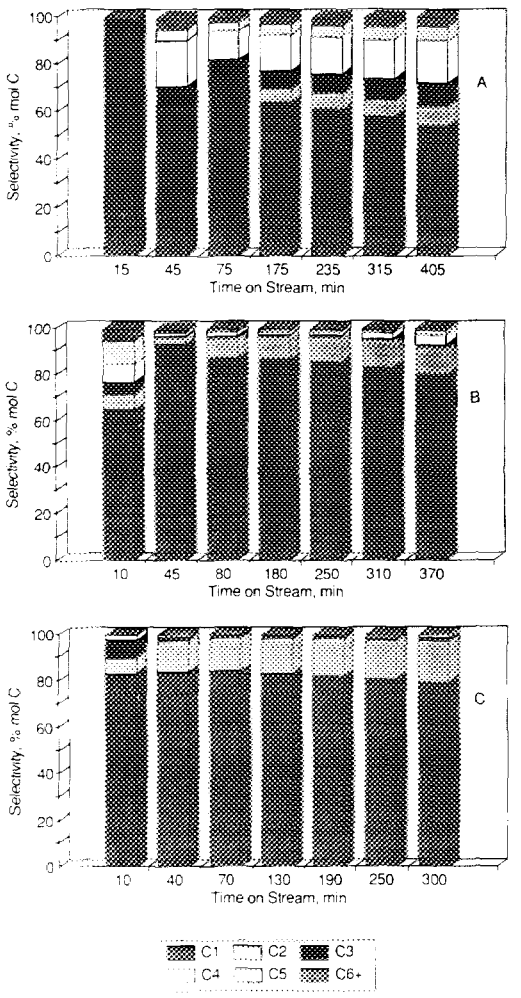

FIG. 5. Change in hydrocarbon distribution of CO hydrogenation over Pd_9Co_9 500/H_2O/500, 500/500, and 500/500/NaOH catalysts versus time on stream: (A) 500/H_2O/500, (B) 500/500, and (C) 500/500/NaOH.

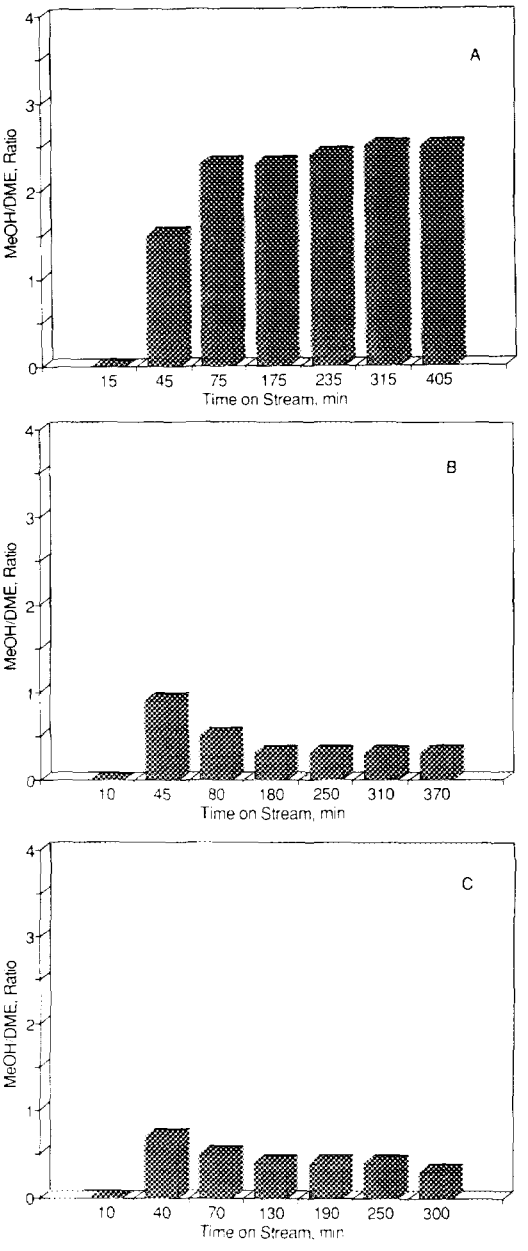

FIG. 6. Change in MeOH/DME ratios in CO hydrogenation over Pd_9Co_9 500/H_2O/500, 500/500, and 500/500/NaOH catalysts versus time on stream: (A) 500/H_2O/500, (B) 500/500, and (C) 500/500/NaOH.

c. 500/500/NaOH Catalyst

The 500/500/NaOH catalyst is very active initially, but deactivates rapidly, as illustrated in Fig. 3. Its steady-state activity is very close to that of the 500/H_2O/500 catalyst; within 22 h it drops to nearly 1/10 of the initial value. Still, the activity of 500/500/NaOH at this stage is higher than that of the deactivated 500/500 catalyst. In addition, the selectivity of the 500/500/NaOH catalyst parallels that of the 500/500 catalyst (Fig. 4). After 22 h, the selectivity for oxygenates is about 20% for 500/500/NaOH, while that of the 500/500 catalyst at the same TOS is nearly zero. The hydrocarbons are

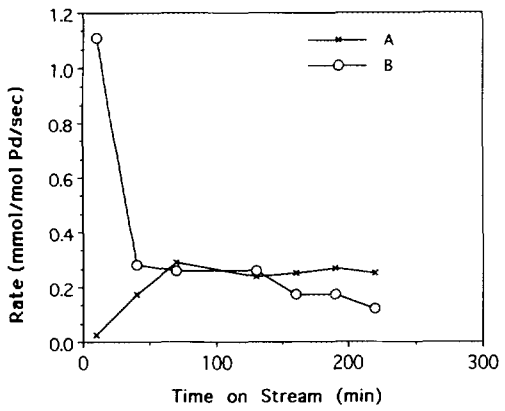

FIG. 7. Change in conversion rate of CO hydrogenation over Pd_9 500/H_2O/500 and 500/500 catalysts versus time on stream: (A) 500/H_2O/500 and (B) 500/500.

richer in C_{4+} for 500/500/NaOH than for the 500/500 catalyst at a TOS of 22 h. The low MeOH/DME ratio with the 500/500/NaOH resembles that of the 500/500 catalyst.

d. Pd_9/500/H_2O/500 and Pd_9/500/500 Catalysts

The Co-free Pd_9NaY catalysts are examined after calcination and reduction at 500°C. As shown in Fig. 7, the initial activity of Pd_9/500/500 is higher than that of the Pd_9/500/H_2O/500 catalyst, but the former deactivates faster than the latter. Remarkably, the steady state activity of the Pd_9Co_9/NaY catalyst is 2–4 times higher than that of the corresponding Co-free Pd_9 catalysts. A significant difference in selectivity to oxygenates is found between Pd_9Co_9 and Pd_9 after the same 500/500 pretreatment (see Fig. 4 and Fig. 8). The selectivity of the Pd_9 catalyst shifts rapidly from methane to MeOH + DME and then to C_{2+}, as shown in Fig. 8. Such shifts are accomplished within 90 min. The steady state selectivity and hydrocarbon distribution do not differ much between these two catalysts.

e. X-ray Diffraction

As shown in Table 1 and Figs. 9–12, the reduced metal particles are initially too small to be detected in XRD, in agreement with previous results (*12*). However, after some time on stream most catalysts display XRD patterns, indicative of significant agglomeration of metal particles. Simultaneously some disintegration of the zeolite structure is observed. The metal present in all $T_C/H_2O/T_R$ catalysts is monophasic, either Pd carbide for T_R = 250°C, or a PdCo alloy for T_R = 500°C; the particles are 6 nm large. Catalysts that were not exposed to H_2O vapor prior to reduction give no discernible Pd(111) diffraction, indicating highly dispersed Pd particles, (traces B in Fig. 9 and 10). However, the 500/250 and 500/500 catalysts display coexistence of PdC and Pd phases after reaction for 20–24 h; the Pd particles are fairly large, but the Pd carbide particles are much smaller (traces D in Fig. 9 and E in Fig. 10). The striking difference between the 500/H_2O/500 and

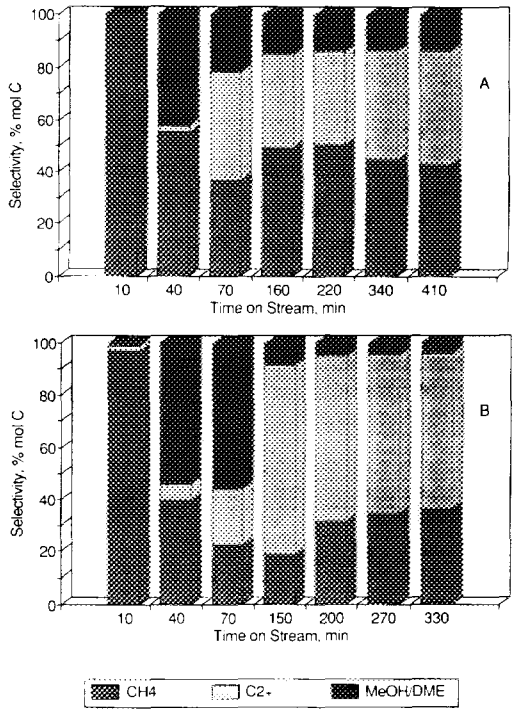

FIG. 8. Change in selectivity in CO hydrogenation over Pd_9 500/H_2O/500 and 500/500 catalysts versus time on stream: (A) 500/H_2O/500 and (B) 500/500.

TABLE 1

XRD Results on Mean Particle Sizes and Line Position

Peak Cat.	Pd	PdC	PdCo	2θ and ratio[a]
500/H_2O/250 (6 h)	—	6.3 nm	—	39.42°
500/H_2O/500 (7 h)	—	—	5.8 nm	40.73°
500/250 (22 h)	33.6 nm	4.6 nm	—	39.87° 40.17° R = 1.9
500/500 (6 h)	—	—	—	Too weak and diffuse
500/500 (22 h)	36.3 nm	4.6 nm	—	39.97° 40.19° R = 0.8
Pd_9NaY-I[b] (22 h)	11.3 nm	—	—	39.16°
Pd_9NaY-II[b] (6 h)	15.5 nm	12.6 nm		39.12° 40.03° R = 0.64
500/500/NaOH (6 h)	—	—	10.4 nm	40.53°
500/500/NaOH (22 h)	—	—	3.4 nm	40.75°

[a] Ratio R is the intensity ratio of PdC/Pd; the two 2θ values, if presented in the same cell, refer to the peak positions of the PdC(111) and Pd(111) reflections, respectively.

[b] All other catalysts without specifying composition are Pd_9Co_9/NaY catalysts, for Pd_9NaY, I denotes Series I (with rehydration), and II, Series II (without rehydration).

500/500 catalysts after TOS of 6 h is displayed in Fig. 10: while PdCo alloy diffraction peaks are clearly observed for 500/H_2O/500 (trace D), the 500/500 catalyst shows a barely discernible Pd carbide (111)

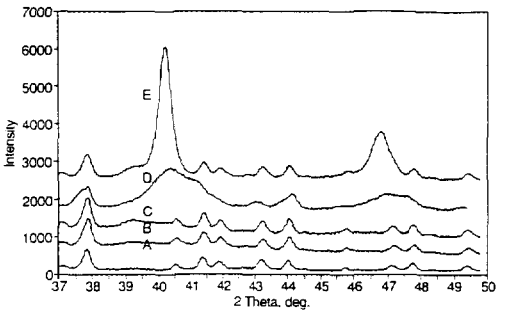

FIG. 10. X-ray diffraction pattern of Pd_9Co_9 catalysts with T_C = 500°C and T_R = 500°C after CO hydrogenation at 250°C.

diffraction (trace C). Interestingly, the neutralized Pd_9Co_9 500/500/NaOH catalyst shows exclusively a PdCo alloy phase after 6 h on stream (Fig. 11). The XRD peak characterizing Pd–Co alloy particles of the neutralized catalyst after 22 h (trace C in Fig. 11) is definitely of higher intensity and of narrower FWHM, and located at higher 2θ than after 6 h on stream (trace E in Fig. 11). Evidently, this shows that for the neutralized sample the PdCo alloy particles grow in size and number with extended time on stream, and they become richer in Co.

For the Pd_9/500/500 catalyst, a small Pd carbide peak and a peak of Pd metal are detected by XRD as shown in Fig. 12 (trace B). In contrast, only reflections from the Pd

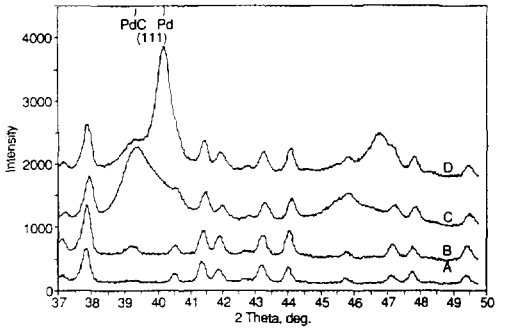

FIG. 9. X-ray diffraction pattern of Pd_9Co_9 catalysts with T_C = 500°C and T_R = 250°C after CO hydrogenation at 250°C.

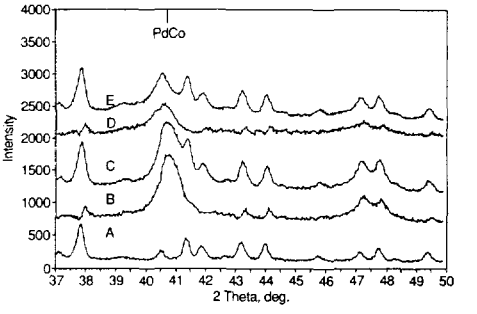

FIG. 11. X-ray diffraction pattern of Pd_9Co_9 500/500/NaOH after CO hydrogenation at 250°C for different times on stream.

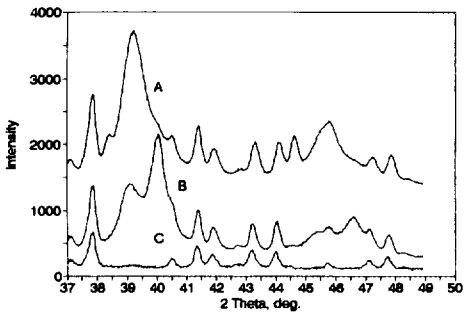

FIG. 12. X-ray diffraction pattern of Pd_9 catalysts with T_C = 500°C and T_R = 500°C after CO hydrogenation at 250°C.

carbide exist in the XRD pattern of the 500/H_2O/500 catalyst; see trace A in Fig. 12.

The deconvolution results for the (111) peaks of Pd_9Co_9/500/250, Pd_9Co_9/500/500, and Pd_9/500/500 catalysts are shown in Fig. 13 as (A), (B), and (C), respectively. The (200) peaks for corresponding catalysts give compatible results of deconvolution (not shown).

The XRD results are summarized in Table 1. The values in parentheses in the first column show the time-on-stream history of the catalysts.

IV. DISCUSSION

Our recent work on zeolite-supported bimetal catalysts revealed that location, ligancy, and reducibility of metal ions, as well as the particle size and phase composition of reduced metal particles are crucially determined by parameters such as the calcination and reduction programs (*8–14*). The present paper shows that an additional parameter, i.e., rehydration during the interval between calcination and reduction, has a pronounced effect on the active bimetal phases and thus also on activity and selectivity of the catalysts.

This effect is rather small for the samples reduced at 250°C. The 500/H_2O/250 and 500/250 catalysts are similar in steady-state activity and selectivity; differences in hydrocarbon distribution are small. After CO hydrogenation the Pd carbide phase prevails in monometallic Pd/NaY catalysts (*12*). The overwhelming similarity of Pd_9Co_9 and Pd_9 500/H_2O/250, both in catalytic signature and as to the nature of the active metal phases, suggests that Co^{2+} ions remain mostly unreduced at 250°C. Rehydration of the Pd_9Co_9 catalyst precursor has only a negligible effect on the reduction of Co^{2+} ions, it does not affect the state of Pd carbide. A Pd phase is present in these samples, but the Pd particles are very large (33.6 nm, Table 1) so that

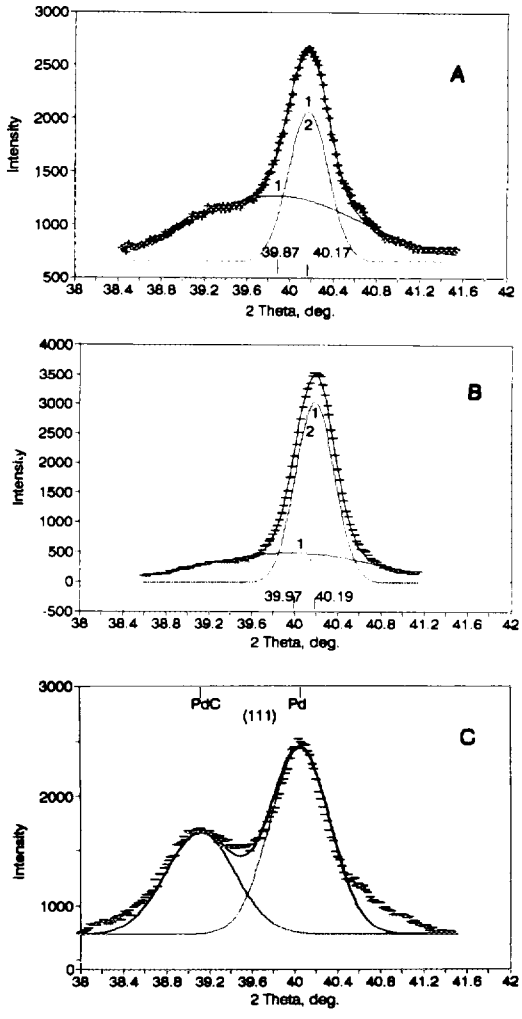

FIG. 13. Deconvolution of (111) peaks: (A) Pd_9Co_9/500/250, (B) Pd_9Co_9/500/500, and (C) Pd_9/500/500.

Pd metal does not contribute much to the catalytic performance of the catalyst. Instead, Pd carbide particles of an average size of 4.6 nm will dominate catalytic activity. The same holds for the 500/H_2O/500 catalyst with PdC_x particles of 6.3 nm.

The Pd_9Co_9 catalysts 500/H_2O/250 and 500/250 differ significantly in initial activities and in the nature of the final metal phase. In order to interpret these effects we assume that transition metal ions form aequo-complexes and, consequently, become mobile. For Pd/NaY we found that rehydration of Pd^{2+} ions after calcination leads to large Pd particles upon reduction (*15*). Monoatomically dispersed Pd in NaY can only be formed by reduction immediately following calcination (*16*). In the PdCo bimetal catalysts, rehydration of Co^{2+} ions should also be considered. Even though the reduction of Co^{2+} ions in both catalysts is negligible at low temperature, the difference in the location of Co^{2+} ions is likely responsible for these observed differences. After calcination at 500°C, most Co^{2+} ions are located in hexagonal prisms, and some are in sodalite cages. Subsequent water exposure leads to migration of Co^{2+} ions to supercages where they form stable $[Co(H_2O)_6]^{2+}$ complexes. Without solid experimental data, the present authors refrain from speculation on the causes of the difference in the metal phases of the catalyst 500/H_2O/250 and 500/250 after reaction. However, in view of the production of water molecules during CO hydrogenation, the conclusion is evident that water exposure *prior to reduction* has the most significant effect on the metal phases and the activity pattern of the catalysts.

The effect of exposure to water vapor is most striking for samples that were calcined and reduced at 500°C. Two samples of identical composition (9 Co and 9 Pd atoms per unit cell) differ in product distribution, rate of deactivation and phases identified by XRD. As to product distribution, the 500/500 sample shows a catalytic signature reminiscent of monometallic Pd/NaY with oxygenates prevailing, after a brief induction period where much methane is formed, precisely as for Pd/NaY. After 22 h on stream this catalyst deactivates, and no PdCo alloy particles are detected by XRD; only Pd carbide particles of medium size and large Pd particles are identified. The Pd_9Co_9 500/H_2O/500 catalyst displays a strikingly different product pattern: methane prevails at all times, followed by higher hydrocarbons. This sample thus has the signature of a Fischer–Tropsch catalyst. After reaction, a PdCo alloy phase is detected by XRD, but no Pd carbide is found. From the XRD data we estimate that the alloys contain 10–20 at% Co. These alloy particles are of nearly similar size as the Pd carbide particles in the 500/500 catalyst. They are much larger than the supercages; presumably they cause local destruction of the zeolite structure and form voids, as reported by Jaeger *et al.* (*17*).

Previously it was found that the reduction of Co^{2+} ions increases at higher temperature, once Pd^{2+} and Co^{2+} meet the proximity requirement (*8*). For the 500/H_2O/500 and 500/500 catalysts, two different reduction scenarios are expected. In the 500/H_2O/500 catalyst, the decisive effect is the formation of a mobile cobalt aequo complex (*18, 19*). This induced mobility enables the $[Co(H_2O)_6]^{2+}$ ions to migrate towards the palladium ions. Presence of both elements in the supercage network will facilitate formation of alloy particles during catalyst reduction. As a consequence, alloy particles of medium size containing more Co will be obtained. In related work, we observed that exposure of oxidized Pd/HY to NH_3 gas leads to the formation of mobile $Pd(NH_3)_4^{2+}$ complexes that migrate through the supercage channels (*20*).

The suggestion that exposure of the calcined catalyst precursor to H_2O vapor transforms Co^{2+} ions, initially in hexagonal prisms and sodalite cages, into $[Co(H_2O)_6]^{2+}$ ions, located in supercages, is supported by the observed change in color. After calcination to 500°C, the sample is purple-blue, indicating tetrahedral coordination of the

Co^{2+} ions by framework oxygen atoms. This strong color dominates over the pink color of the Pd^{2+} ions. After extended exposure to H_2O vapor, the color changes to pink indicating formation of $[Co(H_2O)_6]^{2+}$ ions. It can thus be concluded that complexation of the metal ions and migration of the aequocomplexes prior to reduction has the most significant effect in determining the metal phases and activity pattern of the catalysts.

For the 500/500 catalyst, however, Pd^{2+} and Co^{2+} ions share sodalite cages. Reduction might produce small PdCo alloy clusters in sodalite cages, but subsequent oxidative "*leaching*" by zeolite protons will reoxidize the Co atoms of such alloy particles. Such proton leaching of one component out of zeolite supported bimetal particles has been found previously for PtCu (*21*), PdCu (*22*), and PdNi (*23*). One could imagine that this process is mediated by physisorbed water. It is possible that the Co^{2+} ions then act as anchors for the Pd particles. This mechanistic view can account for the stabilization of Pd particles under CO hydrogenation even after 6 h on stream (trace C, Fig. 10). On the other hand, PdCo alloy particles of 5.8 nm prevail for $500/H_2O/500$ under steady state. Co leaching from these PdCo alloy particles by protons at remote sites is obviously not feasible. The drastic decrease in activity for the 500/500 catalyst after 22h (Fig. 3) is clearly related to the drastic increase in size of the Pd metal particles. This could be a consequence of de-anchoring, as Co^{2+} ions, that tie Pd particles to cage walls, slowly migrate from supercages to hidden sites during the course of reaction. The large Pd particles evidenced by XRD are indicative of such mechanism.

The coexistence of many small and some very large metal particles has been confirmed recently by TEM pictures (not shown) of the 500/500 catalyst after a TOS of 6 h. The XRD results show that the large particles consist of Pd; the composition of the encaged small metal particles is still under investigation. It is possible that a small concentration of Co in either the Pd metal or the Pd carbide particles, or an interaction of these particles with Co^{2+} ions results in a catalyst promotion effect, analogous to that reported by Choudary *et al.* for PdFe/NaX and Pd/SiO_2 catalysts (*4*). These authors showed that a very low concentration of Fe ($\approx$0.07 atomic fraction) exerts a promotional effect for oxygenate formation in CO hydrogenation. In this case the formation of a PdFe alloy was detected by Mössbauer spectroscopy. Co^{2+} ions interacting with Pd particles in zeolites are likely to act not only as catalyst promoters but also as chemical anchors. The high activity for oxygenates of the prevailing small metal particles in the Pd_9Co_9 500/500 catalysts is tentatively attributed to the combined effects of anchoring and promotion by Co. The composition of the small particles in this catalyst is still uncertain; we are fairly sure, however, that the Co/Pd ratio in them is very low. In contrast, the catalysts which were exposed to H_2O prior to reduction contain alloy particles, fairly rich in Co, as the active phase and produce C_{2+} hydrocarbons.

The conclusion that the observed dramatic effect of H_2O is primarily an effect on the Co^{2+} ions, is confirmed by the relatively modest changes which H_2O exposure induces on cobalt-free Pd_9NaY catalysts. Comparisons of $Pd_9/500/H_2O/500$ and $Pd_9/500/500$ catalysts reveals that both produce initially CH_4, which is indicative for the dissociative chemisorption of CO on small Pd particles. Once Pd carbide has been formed, oxygenates prevail over both catalysts. When the metal carbide particles grow, the ratio of metal to acid sites decreases; consequently secondary reactions of oxygenates to heavier hydrocarbons dominate the product composition. The only remarkable effect of H_2O exposure on the Pd samples is the different activity in the first 10 min, for which we do not offer an explanation.

The results consistently show that the composition of the reduced particles immediately after reduction is strongly dependent

on the success of driving Co^{2+} ions out of the hidden cages and mobilizing them by adding water ligands. Alloy particles will, however, lose part of the Co, if *leaching* by zeolite protons is significant. In this respect, comparison of the Pd_9Co_9 500/500 catalyst with its neutralized counterpart, $Pd_9Co_9$500/500/NaOH is relevant. The results show that the catalytic performance of both catalysts is similar, although the lack of protons impairs secondary reactions; by consequence the MeOH/DME ratio is higher in the neutralized catalysts. The XRD data show that after several hours on stream rather large PdCo particles are formed in the neutralized catalyst. It is even possible to estimate their composition from the lattice spacing: 11 at% Co after 6 h and 22% Co after 22 h. This agglomeration explains the decrease in activity with TOS. It may also indicate that the anchoring action of protons or Co^{2+} ions produced by proton leaching is beneficial for maintaining a reasonable dispersion. As neutralization with NaOH was done in aqueous solution after reduction, the data illustrate, again, the importance of water exposure *before* reduction of the ions for obtaining the dramatic changes in selectivity discussed above.

In summary, the picture emerging from the present data is that exposure to H_2O vapor of the calcined catalyst precursor leads to formation of complexed ions in zeolite supercages and thus increased mobility for both Pd and Co ions. The migration of Co^{2+} ions from hidden sites to supercages is essential for their reducibility. As a consequence, the rehydrated samples contain, after reduction in hydrogen, alloy particles of medium size which are much richer in Co than the metal particles in catalysts that were reduced immediately after calcination. This difference in alloy composition is the major cause for the rather dramatic differences in catalytic behavior. The 500/H_2O/500 catalyst is a Fischer–Tropsch catalyst directing CO hydrogenation mainly to hydrocarbons. The bimetal catalysts 500/500 and 500/500/NaOH contain Pd or Pd carbide particles, possibly some alloy particles lean in Co. They display a high selectivity for oxygenates and their secondary products.

ACKNOWLEDGMENTS

We gratefully acknowledge support from the Director of the Chemistry Division, Basic Energy Science, U.S. Department of Energy, Grant DE-FG02-87ERA13654.

REFERENCES

1. Sachtler, W. M. H., Shriver, D. F., Hollenberg, W. E., and Lang, A. F., *J. Catal.* **92,** 429 (1985).
2. Van den Berg, F. G. A., Glezer, J. H. E., and Sachtler, W. M. H., *J. Catal.* **93,** 340 (1985).
3. Niemantsverdriet, J. W., Louwers, S. P. A., van Grondelle, J., van der Kraan, A. M., Kampers, F. W. H., and Koningsberger, D. C., *in* "Proceedings, 9th International Congress on Catalysis, Calgary, 1988" (M. J. Phillips and M. Ternan, Eds.), Vol. 2, p. 674. Chem. Institute of Canada, Ottawa, 1988.
4. Choudary, B. M., Lázár, K., Matusek, K., and Guczi, L., *J. Chem. Soc., Chem. Commun.*, 592 (1988).
5. Choudary, B. M., Lázár, K., Bogyay, I., and Guczi, L., *J. Chem. Soc., Faraday Trans. I* **86,** 419 (1990).
6. Uytterhoeven, J. B., *Acta Phys. Chem.* **24,** 53 (1978).
7. Kim, J. C., and Woo, S. I., *Appl. Catal.* **39,** 107 (1988).
8. Zhang, Z., Sachtler, W. M. H., and Suib, S. L., *Catal. Lett.* **2,** 395 (1989).
9. Zhang, Z., and Sachtler, W. M. H., *J. Chem. Soc., Faraday Trans.* **86,** 2312 (1990).
10. Feeley, J. S., and Sachtler, W. M. H., *Zeolites* **10,** 738 (1990).
11. Yin, Y.-G., Zhang, Z., and Sachtler, W. M. H., *J. Catal.* **138,** 721 (1992).
12. Cavalcanti, F. A. P., Dossi, C., Sheu, L. L., and Sachtler, W. M. H., *Catal. Lett.* **6,** 289 (1990).
13. Cavalcanti, F. A. P., Stakheev, A. Yu, and Sachtler, W. M. H., *J. Catal.* **134,** 226 (1992).
14. Zhang, Z., Chen, H., and Sachtler, W. M. H., *J. Chem. Soc. Faraday Trans.* **87,** 1413 (1991).
15. Zhang, Z., Mestl, G., Knözinger, H., and Sachtler, W. M. H., *Appl. Catal.* **89,** 155 (1992).
16. Zhang, Z., Chen, H., Sheu, L. L., and Sachtler, W. M. H., *J. Catal.* **127,** 213 (1991).
17. Jaeger, N. I., Jourdan, A. L., Schulz-Ekloff, and Svensson, A., *in* "Structure and Reactivity of Surfaces" (C. Morterra, Z. Zecchina, and G. Costa, Eds.), p. 503. Elsevier, Amsterdam, 1989.

18. Klier, K., *Langmuir* **4,** 13 (1988).
19. Hutta, P. J., and Lunsford, J. H., *J. Chem. Phys.* **66,** 4716 (1977).
20. Feeley, O., and Sachtler, W. M. H., *Appl. Catal.* **67,** 141 (1990).
21. Tzou, M.-S., Kusunoki, M., Asakura, K., Kuroda, H., Moretti, G., and Sachtler, W. M. H., *J. Phys. Chem.* **95,** 5210 (1991).
22. Zhang, Z., Xu, L., and Sachtler, W. M. H., *J. Catal.* **131,** 502 (1991).
23. Feeley, J. S., and Sachtler, W. M. H., *J. Catal.* **131,** 573 (1991).